Preprint
UCRL-JC-138649

Model-Based Nonrigid Motion Analysis Using Natural Feature Adaptive Mesh

Y. Zhang, D.B. Goldgof, S. Sarkar and L.V. Tsap

This article was submitted to
International Conference on Pattern Recognition, Barcelona, Spain,
September 3-8, 2000

U.S. Department of Energy

Lawrence
Livermore
National
Laboratory

April 25, 2000

Model-Based Nonrigid Motion Analysis Using Natural Feature Adaptive Mesh

Yong Zhang, Dmitry B. Goldgof and Sudeep Sarkar
Department of Computer Science & Engineering
University of South Florida
Tampa, FL 33620
zhang, or goldgof, or sarkar@csee.usf.edu

Leonid V. Tsap
Center for Applied Scientific Computing
Lawrence Livermore National Laboratory
Livermore, CA 94551
tsap1@llnl.gov

Abstract

The success of nonrigid motion analysis using physical finite element model is dependent on the mesh that characterizes the object's geometric structure. We suggest a deformable mesh adapted to the natural features of images. The adaptive mesh requires much fewer number of nodes than the fixed mesh which was used in our previous work. We demonstrate the higher efficiency of the adaptive mesh in the context of estimating burn scar elasticity relative to normal skin elasticity using the observed 2D image sequence. Our results show that the scar assessment method based on the physical model using natural feature adaptive mesh can be applied to images which do not have artificial markers.

1 Introduction

During the past two decades, the study on nonrigid motion has evolved following the vein of adding more constraints on various motion estimation methods [1] [3]. Methods without an object model impose minimum constraints on the tracking process, but require efficient search and comparison throughout the entire image. By adding kinematic continuity constraints on the object in terms of shape functions, the lumped-parameter model can predict the object's motion in next frame, and thus greatly reduces the tracking complexity. The physical model adds an extra material constraint on the motion computation through the constitutive law [5] [8]. Therefore, the prediction is more accurate and physically sound. The numerical physical model is built by discretizing governing equations over a mesh that covers the object. Mesh serves not only as a computational unit, but also as an implicit topological constraint on the motion, which is very valuable for tracking the elastic body. The meshing schemes used in computer vision research can be classified based on the following criteria:

(1) mesh structure (triangle vs. quadrilateral)
(2) mesh coordinate (image plane vs. scene coordinate)
(3) mesh ROI (whole image domain vs. specific object)
(4) mesh control (feature-first vs. mesh-first)

The quadrilateral mesh is superior to the triangle mesh in terms of its stability performance in the nonlinear system. But in nonrigid motion analysis, unstructured triangle mesh is far more appealing due to its computational efficiency and flexibility in handling complex geometry. Mesh can be constructed either in the image plane or in the scene coordinates. The primary usage of the image mesh is assisting in the apparent motion estimation and video compensation [11]. The scene mesh is commonly used to build a numerical physical model, and usually covers only the isolated object of interest. Either the feature-first scheme or the mesh-first scheme can be used to generate a mesh that is adaptive to the image content, which may or may not have artificial markers.

This work is a further advancement of the previous investigations on finding an objective method for burn scar assessment [9]. Our previous work was carried out on images attached with artificial markers and the fixed mesh. By constructing a mesh adaptive to natural features, we extend the applicability of the method to images without artificial markers, and also increase the computational efficiency.

2 Model Based Object Reconstruction

In the framework of the model-based object reconstruction, three stages are involved: (1) model construction, (2) model calibration and (3) model prediction (Figure 1). Various types of object's attributes can be estimated in three stages: structure, motion and material properties.

Two important steps in building a numerical model are to generate an accurate mesh and to determine the appropriate boundary conditions, In this study, we emphasize on generating an adaptive mesh using the feature-first scheme.

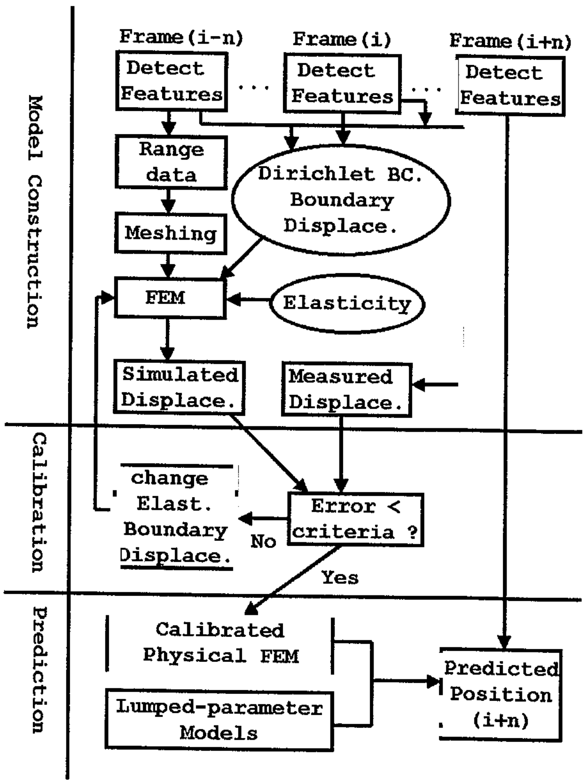

Figure 1. Illustration of the physical model-based object reconstruction.

Before a model can be used for making predictions, it must be calibrated against the observations to adjust its parameters. In this way, model-based object reconstruction problems will be eventually transformed into parameter estimation problems, which are often ill-posed in Hadamard sense [2]. Therefore, *a priori* knowledge is needed to overcome the ill-posedness.

Using a calibrated lumped-parameter model, $\mathbf{P}_{i+1} = \mathbf{M}_i\mathbf{P}_i + \mathbf{T}$, the object's position $\mathbf{P}_{i+1}$ can be computed from the past motion trajectory $(\mathbf{M}_i, \mathbf{P}_{i-1}, ...)$. Therefore, it reflects the object's *kinematic* continuity. As an excitation driven system, the calibrated physical model makes predictions as a response to external forces. The prediction reflects the continuity of the object's *dynamic* status. We used transient elastic model, $\mathbf{M}\ddot{\mathbf{x}} + \mathbf{D}\dot{\mathbf{x}} + \mathbf{K}\mathbf{x} = \mathbf{F}(t)$, to compute displacement vector $\mathbf{x}$ as a result of repeated force inputs $\mathbf{F}(t)$, or inertial motion driven by mass matrix $\mathbf{M}$. The solution was constrained by stiffness matrix $\mathbf{K}$ and damping matrix $\mathbf{D}$. We also utilized the kinematic data to specify the Dirichlet condition of the physical model. Hence, the physical model and the lumped-parameter model were used to track the nonrigid motion in a cooperative way.

3 Model Construction: Adaptive Mesh

Natural Feature Points Selection Feature points suitable for object representation and motion tracking can be found by computing eigenvalues $(\lambda 1, \lambda 2)$ of the 2×2 gradient matrix of a small feature window [6]. A window possessing the relationship of $\min(\lambda 1, \lambda 2) > \lambda$ will be considered as a candidate, where λ is a user specified threshold value.

As shown in Figure 2 (a) and Figure 3 (a), most of the selected points captured the significant features, such as natural birthmarks and artificial markers. An ideal set of feature points for a deformable mesh should have a balanced distribution on the object's surface. We used another threshold d, the minimum distance between any two adjacent feature points, to control the feature distribution. The locally adaptive assignment of λ and d also helped to generate a set of points with the desired quality.

Feature-First Meshing Scheme Two meshing schemes are frequently used in the computer vision research: the mesh-first and the feature-first. In the feature-first scheme, after features being extracted, the mesh can be constructed adaptively based on the feature distribution. The advantage of the feature-first scheme is that it is applicable to a large variety of images, particularly those with objects of complex shapes. The disadvantages are the sophisticated algorithms involved and the dependence of the mesh quality on the feature quality.

Given a set of randomly distributed feature points, various triangle mesh can be produced by linking points following certain selection and rejection rules. We used the Delaunay principle to generate the triangle mesh [7]. In a Delaunay triangle mesh, no vertex will be allowed to sit inside the circumscribing circle of any element. An algorithm obeying the Delaunay principle can yield a mesh adaptive to the original set of vertex. However, it does not necessarily guarantee a mesh with desired geometrical quality, and thus the refinement must be performed to insert new nodes into the mesh. In this study, we allowed new nodes to be added in both 2D image mesh and 3D scene mesh. In the former case, the addition of new nodes was achieved during the feature extraction stage. The node addition in 3D scene mesh was done in the postprocessing stage of mesh generation as a quality assurance procedure. Figure 2 shows two mesh examples with and without the refinement.

In addition to the geometrical consideration of mesh quality mentioned above, another strong motivation for the adaptive refinement is to capture the dramatic change of modeling parameters in a small region where the severe deformation occurs. The refinement process can be driven by minimizing the error function between two consecutive simulations of the physical model. In our experiment, new nodes were added at the boundary between the normal skin

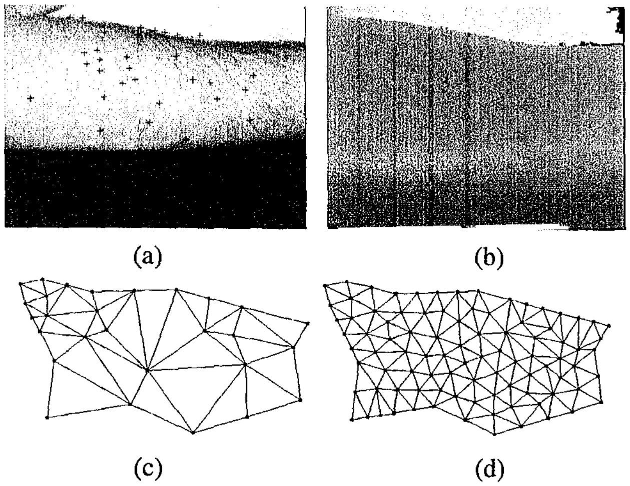

Figure 2. Triangle meshes generated using the feature-first scheme. (a) Intensity image (feature points cross-marked). (b) Range image. (c) Triangle mesh on the original point set. (d) Triangle mesh with new nodes added.

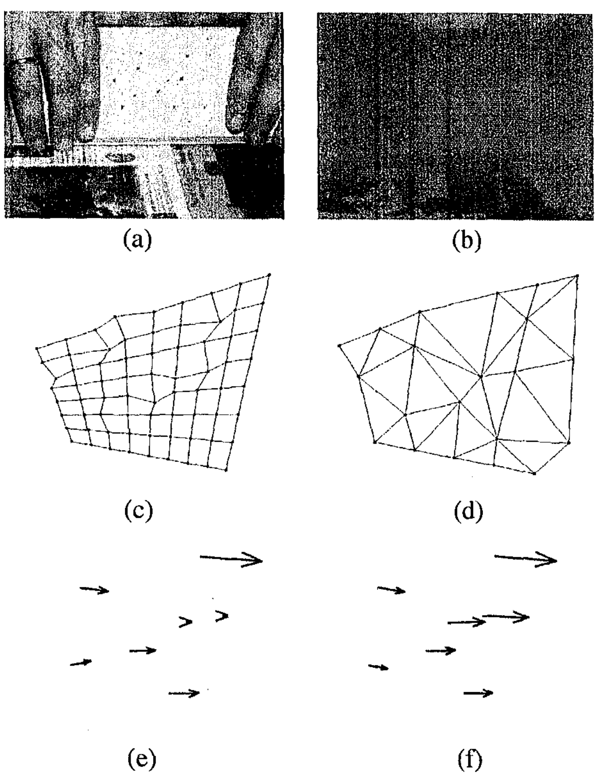

Figure 3. The comparison of meshes using the feature-first and the mesh-first schemes. (a) Intensity image (selected features are marked). (b) Range image. (c) Quadrilateral mesh. (d) Triangle mesh. (e) Recovered motion using quadrilateral mesh. (f) Recovered motion using triangle mesh.

and the burn scar, where elasticity showed significant variations and large simulation errors.

Mesh-First Meshing Scheme The mesh-first scheme has the advantage of being easy to implement. After a regular mesh is defined (usually quadrilateral), a simple post-processing can be performed to reshape the mesh to match feature points. This scheme is useful for the image where objects can be tagged by the invasive or noninvasive markers [4] [10]. The obvious drawback is that not all images can be attached with artificial markers. In addition, the initial mesh can not be stretched to a degree that original mesh structure is destroyed, and thus no longer suitable for the nonrigid motion tracking.

Figure 3 (c) shows an adaptive quadrilateral mesh after being adapted to the underlying feature points. The object in the image is an elastic bandage (with artificial markers) under stretching. Figure 3 (d) shows a triangle mesh generated using the feature-first scheme. Figure 3 (e) and (f) show that physical models using the quadrilateral mesh and the triangle mesh produced similar results. However, for a large scale simulation, the computational burden caused by the large number of nodes in the quadrilateral mesh is a major concern (to catch a few scattered features, very dense mesh is needed at the expense of many empty nodes).

4. Model Calibration: Parameter Estimation

We explicitly coupled a physical model and an optimization package to take advantage of the fact that an efficient finite element model was already available and could be used with minor modification. After being given the initial guesses of the elasticity and the displacement at the boundary, the forward finite element model run within the optimization loops, during which the elasticity and the displacements were adjusted until the error between the simulated displacements and the measured displacements (at the chosen internal nodes) was less than a predefined tolerance. We also incorporated *a priori* knowledge into the optimization process to alleviate the ill-posedness, particularly the discontinuous dependence of the solution on the measured data, which is stated as the the third condition of ill-posedness [2]. For example, the use of average elasticity of the human skin as an initial guess greatly reduced the search time for an optimal solution.

Frequently, the computed strain is used to show the variation of the elastic property of the nonrigid object under deformation. This method is valid when the stress exerted on the object is approximately uniform. In Figure 4, the pulling force on the skin was roughly equal, and thus the computed strain map clearly revealed the difference of the elasticity between the normal skin and the burn scar.

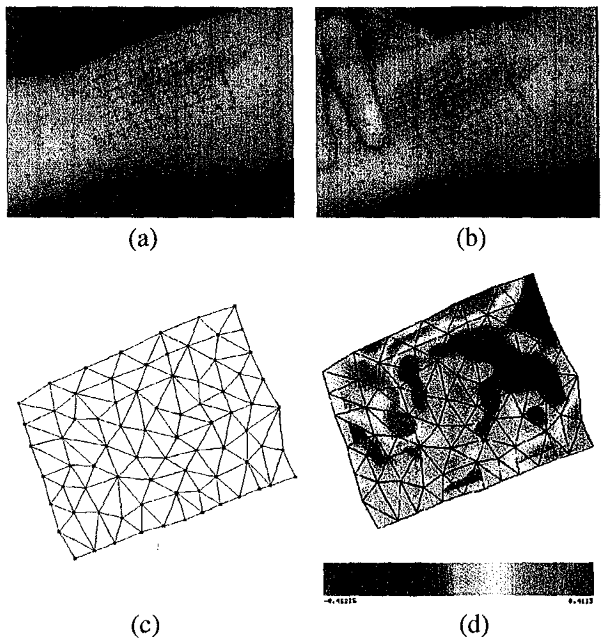

Figure 4. Applications of the adaptive mesh in strain computation and skin property estimation. (a)-(b) The burned skin before/after pulling (feature points are cross marked). (c) Triangle mesh by the feature-first scheme. (d) Computed strain.

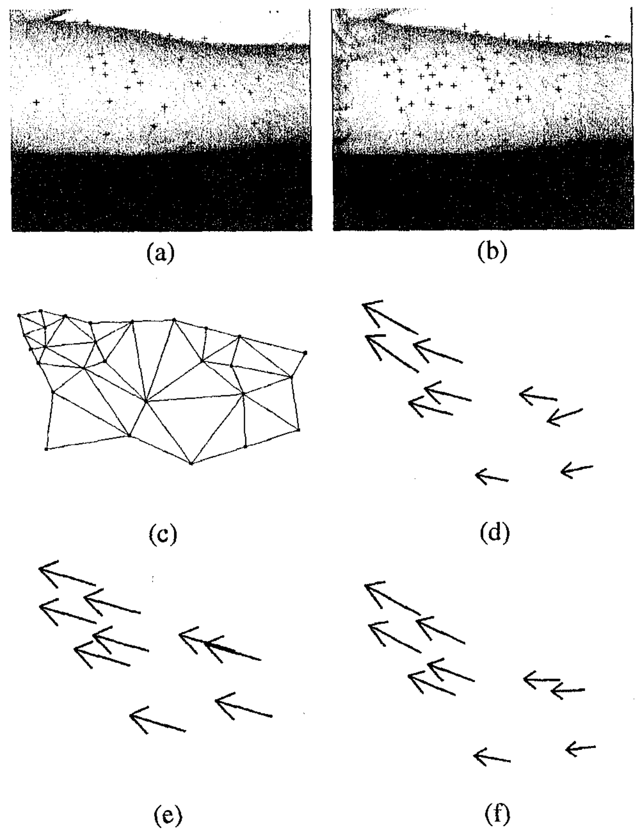

Figure 5. Model based nonrigid motion tracking. (a) The image at t_i (before pulling). (b) The image at t_{i+1} (after pulling). (c) The adaptive triangle mesh. (d) The measured displacements at internal nodes. (e) The initial guesses of displacements by the Hausdorff distance. (f) The final displacements after correction by the physical model.

5. Model Prediction: Motion Tracking

The calibrated physical model can be used in the nonrigid motion tracking because of its unique prediction capability. Predicted displacements could be used in the following ways: (1) as an upper bound for the displacement computed by other methods. (2) as a guideline of the search range for the correspondence in the next frame.

In Figure 5, we demonstrated how the nonrigid motion tracking can be improved by utilizing predictions from the physical model as a correction factor. Figure 5 (a) represents the frame at time i, and Figure 5 (b) the frame at time $i+1$. We assumed that both the elasticity and boundary conditions had been calibrated using the information from previous frames. Dirichlet conditions were specified at the boundary nodes to drive the model. The boundary nodes inherited the old displacement values to make predictions in the next frame, $dx_{(i,i+1)} = dx_{(i-1,i)}$, where dx stands for the displacement. An object experiencing smooth motion will likely to continue to evolve kinematically, even without further external force. Therefore, the above assignment of the boundary condition actually maintained the object's kinematic continuity. But the motion at the internal nodes was constrained by the elasticity, and therefore predictions at those internal nodes reflected the dynamic continuity.

The initial guess of the object's motion between frame i and frame $i+1$ was estimated based on the Hausdorff distance and was plotted in Figure 5 (e). It is clear that only the rigid component exist. After being corrected by the prediction from the physical model, the displacement was almost completely recovered (see Table 1 for the comparison of the recovered motion with the measured motion). It is worth noting that the physical model must be provided with the new displacements to keep the inertia updated (especially for long sequence tracking). Otherwise, the accumulation of small errors in the object's dynamic status will make the further predictions invalid.

6. Conclusions

We have presented a frame work for physical model-based nonrigid motion analysis using the natural feature adaptive mesh. The Delaunay triangle mesh adapted to

	(a)	(b)	error	relative error (%)
point-1	6.185	6.09	0.095	1.5
point-2	3.612	3.98	0.369	10.2
point-3	4.837	5.09	0.252	5.2
point-4	5.135	5.02	0.116	2.3
point-5	3.612	3.29	0.319	8.8
point-6	3.946	3.70	0.245	6.2
point-7	5.977	5.71	0.271	4.5
point-8	4.211	4.02	0.190	4.5
point-9	5.474	5.34	0.132	2.4
average	4.479	4.69	0.221	5.1

Table 1. The comparison of the measured and recovered displacements (mm): (a) The measured data. (b) The recovered data

the natural features can be constructed using the feature-first scheme. The use of the natural feature adaptive mesh provides the following advantages: (1) increasing the computation efficiency of the physical model in simulating the object of complex geometry and, (2) enabling the model to deal with images without artificial markers. We also addressed the issue of the model-guided nonrigid motion tracking in an image stream. Experiments using the human skin as the deformed object indicate that the quality of the nonrigid motion tracking can be improved by utilizing the predictive capability of a physical model.

7. Acknowledgments

This work was partially supported by Biomedical Engineering Research Grant from the Whitaker Foundation and Grant IRI-9619240 from the National Science Foundation. This work was performed under the auspices of the U.S. Department of Energy by University of California Lawrence Livermore National Laboratory under the contract number W-7405-Eng-48.

References

[1] J. K. Aggarwal, Q. Cai, W. Liao, and B. Sabata, "Nonrigid Motion Analysis: Articulated and Elastic Motion", *Computer Vision and Image Understanding*, 70(2), pp. 142-156, 1998.

[2] J. Hadamard, "Lectures on the Cauchy Problems in Linear Partial Differential Equations", *Yale University Press*, 1923.

[3] C. Kambhamettu, D. B. Goldgof, D. Terzopoulos, and T. S. Huang, "Nonrigid Notion Analysis", *Handbook of PRIP: Computer Vision*, Vol. 2, 1994.

[4] S. Kumar and D. Goldgof, "Automatic Tracking of SPAMM Grid and the Estimation of Deformation Parameters from Cardiac MR Images", *IEEE Engineering on Medical Imaging*, 13(1), pp. 122-132, 1994.

[5] A. Pentland and B. Horowitz, "Recovery of nonrigid motion and structures", *IEEE Transactions on Pattern Analysis and Machine Intelligence*, 13(7), pp. 730-742, 1991.

[6] J. Shi and C. Tomasi, "Good Features to Track", *IEEE Conference on Computer Vision and Pattern Recognition (CVPR) Seattle*, June 1994.

[7] S. W. Sloan, "A fast algorithm for constructing Delaunay triangulation in a plane", *Advances in Engineering Software*, 9(1), pp. 34-55, 1987.

[8] D. Terzopoulos and D. Metaxas, "Dynamic 3D models with local and global deformations: Deformable superquadrics", *IEEE Transactions on Pattern Analysis and Machine Intelligence*, 13(7), pp. 703-714, 1991.

[9] L. V. Tsap, D. B. Goldgof, S. Sarkar and P. Powers, "A vision-based technique for objective assessment of burn scars", *IEEE Trans. on Med. Imag.*, 17(4) pp. 620-633 1998.

[10] L. Tsap, D. Goldgof and S. Sarkar, "Nonrigid Motion Analysis Based on Dynamic Refinement of Finite Element Models", *IEEE Conference on Computer Vision and Pattern Recognition (CVPR)*, pp. 728-743, Santa Barbara, CA, June 1998.

[11] Y. Wang and O. Lee, "Use of Two-dimensional Deformable Mesh Structures for Video Coding, Part I - The Synthesis Problem: Mesh-Based Function Approximation and Mapping", *IEEE Transactions on Circuits and Systems for Video Technology.*, 6(6), pp. 636-646, 1996.